16th World Conference on Earthquake, 16WCEE 2017
Santiago Chile, January 9th to 13th 2017
Paper N° 467 (Abstract ID)
Registration Code: S- F1462791097

Centrifuge Model Tests on Failure Behavior of Grid-form Deep Mixing Walls during Large Earthquake

J. Hamada[(1)], T. Honda[(2)]

[(1)] Chief researcher, Research & Development Institute, Takenaka Corporation, hamada.junji@takenaka.co.jp
[(2)] Chief researcher, Research & Development Institute, Takenaka Corporation, honda.tsuyoshi@takenaka.co.jp

Abstract

Grid-form deep cement mixing walls (DMWs) were recently employed to increase bearing capacity of foundations in soft soil as well as a countermeasure against seismic liquefaction. This paper conducted dynamic centrifuge model tests to investigate a failure behavior of DMWs in liquefiable sand during large earthquakes. Two types of models were used for DMWs. One was made of soil-cement with an unconfined compressive strength of about 4,000 kPa. The other was made of acrylic resin that had the same shear stiffness as the initial shear stiffness of soil-cement. The acrylic and soil cement models that supported the rigid weight of 206 kPa were set in a laminar shear box, and repeatedly tested by increasing the acceleration level of the input motion recorded at TAFT earthquakes, in order to investigate the influence of soil-cement's local yielding and failure on seismic performance by comparing it with the seismic response of the acrylic model. It was observed that several cracks were locally induced in the soil-cement model after the maximum input motion of 8.0 m/s^2. The cracks were observed not only in transvers walls but also longitudinal walls. The relatively large cracks at longitudinal walls induced by the inertial force of the structure. However, no significant settlement of the weight was observed even if the normal and shear stresses in the DMWs were assumed to have locally reached the tensile or shear criteria of soil-cement.

Keywords: grid-form deep mixing wall; centrifuge model test; failure of soil-cement; seismic behavior; soil improvement

1. Introduction

Grid-form deep cement mixing walls (DMWs) were recently employed as a new method to increase bearing capacity of foundations in soft grounds as well as a countermeasure against seismic liquefaction. In the method, the high-modulus soil-cement walls confine the loose sand enclosed by DMWs so as not to cause excessive shear deformation during an earthquake. The method was developed in the late 1980s, and has demonstrated that DMWs effectively prevent liquefaction and liquefaction-induced damage in the 1995 Hyogo-ken-Nambu earthquake. During the earthquake, quay walls were heavily damaged due to liquefaction-induced lateral flow. However, a 14-story building with a foundation of cast-in-place concrete piles and DMWs that was surrounded by the quay walls survived the earthquake and no damage was observed in the pile foundation [1]. In Japan, DMWs have been widely used in a lot of buildings since 1995. DMWs have been also applied to support buildings directly, and are capable of restricting the settlement of buildings during or after earthquakes to an acceptable level. Recently piled raft foundations combined with DMWs have been applied to the real buildings. The field measurements on long-term and seismic behaviors of buildings were also performed to confirm the validity of their foundation designs [2, 3].

Some researchers conducted numerical analyses using elasto-plastic models to investigate seismic behaviors of DMWs [4, 5], and concluded that the local failures of DMWs were not the causes of the reduction in the potential for liquefaction mitigation. However, the local failures of DMWs are not acceptable in the existing method of allowable stress design. If a local failure can be appropriately taken into account, DMWs can be designed more rationally, using a performance-based design method. So far, a lot of shaking table tests on cement mixing walls have been carried out by using centrifuges [e.g., 6]. Most of them used acrylic resin models

the shear modulus of which is equivalent to that of real soil-cement in order to investigate an effect of preventing liquefaction during earthquakes. Several researchers recently conducted centrifuge model tests on DMWs using real soil-cement models [7, 8, 9]. Khosravi et al. (2016) used the soil-cement with an unconfined compressive strength of 450 to 770 kPa and investigated the effect of the area replacement ratio and improved depth on the global responses of the soft clay ground. Unfortunately, the above tests were conducted without setting superstructure models on the DMWs. Accordingly, they were not able to reach a conclusion about how the inertial force caused by the superstructure affected DMWs.

This paper conducted a series of centrifuge model tests in the 50 g field in order to investigate failure behaviors of DMWs subjected to dynamic loading from superstructure and ground oscillation during a large earthquake. In this study, a miniature model of DMWs was made of soil-cement in order to investigate the behavior/toughness of the DMWs after yield and failure during a large earthquake. We investigated the relationship between shear stress and shear strain of the DMWs, namely the nonlinearity of the DMWs by gradually increasing the input motion step by step.

2. Centrifuge Model Tests

A series of centrifuge model tests were performed at a centrifugal acceleration of 50 g using a 7 m radius centrifuge at the Takenaka R. & D. Institute. Therefore the scaling ratio was 1/50. Shaking table tests using the acrylic model and soil-cement model were simultaneously carried out to check the shear stiffness and degree of yielding of the soil-cement model. The superstructure was modeled after a low rise building. A series of shaking table tests were conducted with liquefiable sand deposit. However, no liquefaction was observed. This cause will be low water table level (WL = GL-2.5m). So, the water table level at next series of tests was set higher than that in this paper [10]. Silicone oil with viscosity of 50 times that of water is used as pore fluid.

2.1 Setup of model ground, DMWs and structures

Figure 1 shows schematic views of the tests. The DMW models made of soil-cement and acrylic resin were set in a laminar shear box, and a lot of accelerometers, piezometers and displacement transducers were installed on the model, grounds and structures. The inner dimensions of the laminar shear box are 1000 mm long, 300 mm wide, and 350 mm high. A 2 mm-thick membrane was attached to the inside of the box to make it watertight. The size of each DMW model was as follows: 20 mm thick soil-cement wall (1.0 m thick at prototype scale) were spaced 240 mm (12 m at prototype) center-to-center apart from each other as shown in Photo 1. Sand papers were attached, one to the top of the acrylic model and the other to beneath the steel structure models to increase a friction between the structure models and the DMWs.

Silica sand No.6 produced in Iide, Yamagata Prefecture, Japan was used as the soil for all the test cases. The physical properties of the Iide sand are summarized in Table 1. The internal friction angle estimated from consolidated drained tests was 42 degrees at a relative density of 60%. The initial shear modulus of the soil was proportional to the square root of the confining pressure as given in Figure 2, as determined from the initial shear stiffness in a cyclic tri-axial test. The relative density of the saturated model ground is 63 %. Model improved soil-cement walls were also made from Iide sand, kaolin clay and blast-furnace slag cement type B, W/C=60%. Unconfined compressive strength of the soil cement is from 1500 to 2000 kPa at the curing time of 7 days and about 4000 kPa at the curing time of 28 days.

Water table appears at (the depth of) 2.5 m below the ground surface in prototype. Model ground was saturated with 50 cs silicone oil. Each structure model was made of two steel plates whose weight is 11.54kg

plus 16.89 kg, that correspond to a building average contact pressure of 206 kPa. The ground enclosed by DMWs was made by digging the ground about 5 mm deep so as not to contact the raft. Thus, the whole inertial force of the structure can act directly to the DMWs.

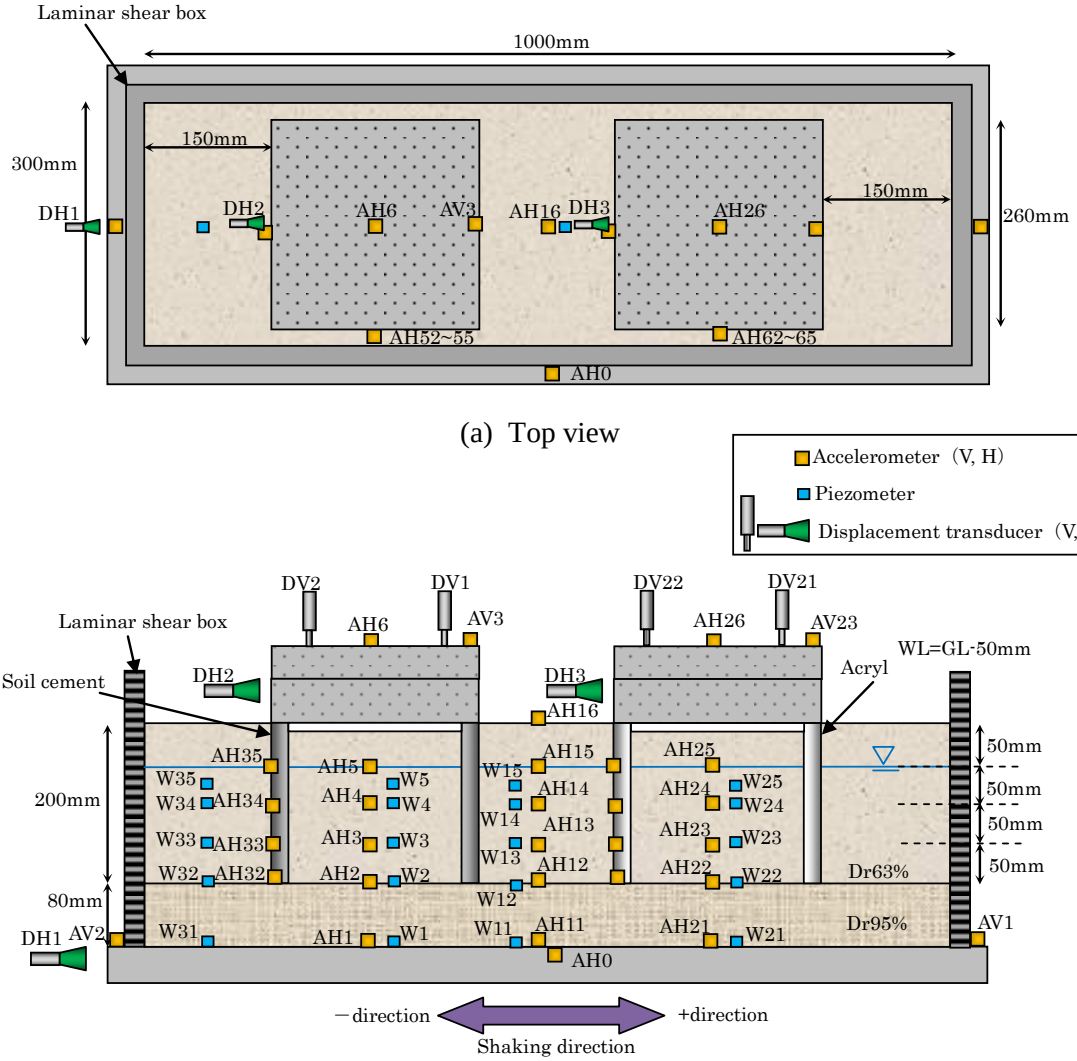

Fig. 1 – Schematic views of models

(a) Soil-cement model (b) Acrylic model

Photo 1 – Deep Mixing Walls models

Table 1 – Physical properties of model (Iide) sand

50 percent diameter	D_{50}	0.28 mm
Uniformity coefficient	U_c	1.9
Specific gravity of soil particles	G_s	2.657
Minimum density	ρ_{dmin}	1.452 g/cm^3
Maximum density	ρ_{dmax}	1.744 g/cm^3

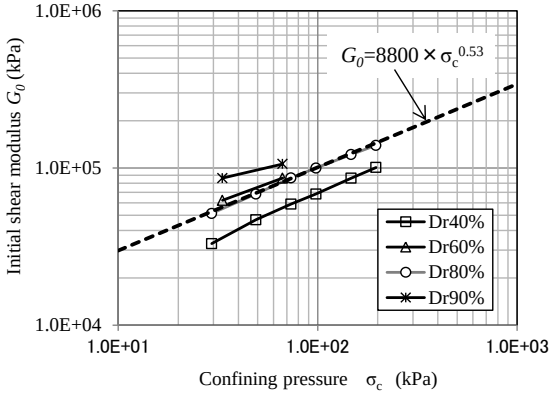

Fig. 2 – Confining pressure versus initial shear modulus of model sand

Table 2 shows the test step numbers and the corresponding peak accelerations at the base (input), ground and structures at each step. Hereafter, test results are converted into the prototype scale. The TAFT wave was used as an input shaking motion throughout the tests. The wave's peak acceleration level was tuned from a small level to a large level, gradually increased step by step. Twenty test steps were conducted in order from above the table. Basically the input (base) accelerations were increased step by step, but several small input waves were provided at the steps 8 and 14 as intermediate steps in order to check the softening degree of the DMWs. If the DMWs were damaged, such a damage should have appeared as a change of natural period of the structure. Highlighting steps of 1, 5, 10, 15 and 18 are analyzed in Figure 7 and 8.

2.2 Test results

Both peak ground accelerations (AH5, AH25) inside the DMWs made of soil-cement and acrylic resin remained almost the same until the step 14 as shown in Table 2. However, those inside the soil-cement DMWs were increased especially at and after the step 15. Table 2 also shows the residual settlements of the models. The

parenthesized values are the integrated values from the beginning of the step 1. The settlements exceeded 100 mm in both the models.

Figures 3 and 4 show the time histories of the measured accelerations and excess pore water pressures respectively, at the step 5. Figures 5 and 6 show those at the step 15 which peak ground acceleration inside the soil-cement DMWs were sharply increased than the one inside the acrylic DMWs. At the step 15, the acceleration inside soil-cement DMWs, AH5, had several sharp peaks after t=5.8 s, where the acceleration of the transverse wall, AH35, made of soil-cement became larger than the longitudinal wall, AH55. The excess pore water pressure inside soil-cement DMWs, W4, was larger than the one inside acrylic DMWs, W24, which however, were not liquefied.

Table 2 – Maximum accelerations and residual settlements (prototype scale)

Step number	Peak Acceleration (cm/s^2)										Residual settlement (mm)							
	Base	Ground			DMWs (Soil-cement)			DMWs (Acryl)			Soil-cement				Acryl			
		inner DMWs (Soil-cement)	inner DMWs (Acryl)	Free field	Transverse	Longitudinal	Structure	Transverse	Longitudinal	Structure								
	AH11	AH5	AH25	AH15	AH35	AH55	AH6	AH45	AH65	AH26	DV2		DV1		DV22		DV21	
1	53	53	56	56	57	49	100	50	52	88	2.3		3.7		1.4		1.5	
2	100	78	78	88	86	78	142	87	76	141	7.3	(9.6)	5.1	(8.8)	4.8	(6.2)	3.5	(4.9)
3	113	94	92	141	95	92	165	104	88	174	3.6	(13.2)	4.7	(13.5)	2.1	(8.3)	3.7	(8.6)
4	140	97	102	128	111	109	185	113	103	200	4.2	(17.4)	3.8	(17.4)	3.4	(11.7)	3.1	(11.7)
5	174	115	120	137	127	121	211	131	122	221	7.6	(25.1)	4.4	(21.7)	4.5	(16.2)	6.3	(18.0)
6	202	136	137	147	151	134	235	143	135	242	5.2	(30.3)	6.8	(28.5)	4.9	(21.1)	6.3	(24.3)
7	245	157	144	165	166	153	248	159	153	269	7.5	(37.8)	6.4	(34.9)	4.6	(25.8)	5.6	(29.9)
8	75	83	122	109	85	77	136	91	72	113	0.3	(38.1)	0.5	(35.4)	0.7	(26.5)	0.2	(30.1)
9	256	178	160	197	198	167	274	188	158	289	6.7	(44.8)	6.7	(42.1)	5.9	(32.4)	5.8	(35.9)
10	333	211	185	219	232	206	300	197	192	311	9.3	(54.1)	7.6	(49.7)	6.7	(39.1)	6.5	(42.4)
11	368	244	226	256	242	211	323	264	217	340	14.0	(68.1)	9.7	(59.4)	5.8	(44.8)	9.3	(51.7)
12	426	292	286	300	274	222	352	307	234	371	11.5	(79.6)	10.7	(70.1)	7.0	(51.9)	5.4	(57.1)
13	407	396	306	323	305	255	379	369	273	396	12.3	(92.0)	9.1	(79.2)	6.6	(58.4)	8.5	(65.6)
14	85	99	84	121	89	82	134	87	76	108	-0.5	(91.4)	0.3	(79.5)	-0.8	(57.7)	-0.2	(65.4)
15	489	793	367	368	412	273	419	457	423	441	11.6	(103.0)	10.1	(89.7)	8.8	(66.5)	9.1	(74.5)
16	530	1288	424	420	534	320	451	536	450	473	11.9	(114.9)	9.0	(98.6)	7.0	(73.5)	7.7	(82.2)
17	635	1288	489	562	643	372	485	487	572	515	9.5	(124.4)	9.4	(108.0)	8.9	(82.3)	11.2	(93.4)
18	715	1176	631	773	820	431	524	607	552	580	13.8	(138.2)	11.6	(119.6)	11.8	(94.1)	12.0	(105.4)
19	832	1289	627	608	821	430	581	732	598	583	8.5	(146.8)	7.1	(126.7)	8.8	(102.9)	9.1	(114.5)
20	581	333	368	346	349	321	423	418	446	384	0.6	(147.4)	1.1	(127.8)	-0.4	(102.5)	1.0	(115.5)

The acceleration response spectra (linear elastic, 5 % damping) to the measured motions in the steps 1, 5 and 15 are shown in Figure 7. At the step 1, the responses of DMWs, AH35, AH55, AH45 and AH65 were almost the same, and the responses correspond to the ground responses enclosed by DMWs, AH5 and AH25. They were amplified to the base acceleration, AH11, and the structure responses were also amplified to those of DMWs. The response of the structure at the soil-cement model was slightly larger than that at the acrylic model in the period range of 0.3-0.9 sec.

At the step 5, the responses of the ground and DMWs were decreased from the base acceleration, and the structure's response at the soil-cement model was almost smaller than that at the acrylic model in the period under 0.5 sec. The responses of DMWs were almost the same as in the step 1.

At the step 15, the responses of transvers wall at both the models, AH35 and AH45, were larger than those of longitudinal wall, corresponding to the ground responses inside DMWs.

Figure 8 shows the acceleration response spectra of DMWs in comparison with those of the ground inside DMWs. At the steps 10 and 15, the response of longitudinal wall at soil-cement model, AH55, was remarkably different from other responses of DMWs for the period under 0.4 sec.

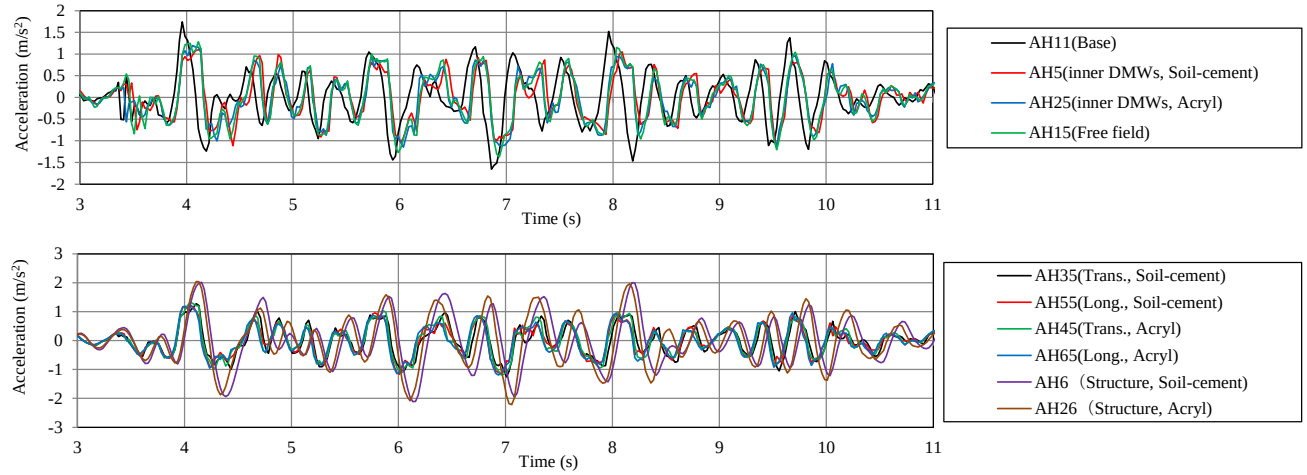

Fig. 3 – Time histories of measured accelerations (step 5)

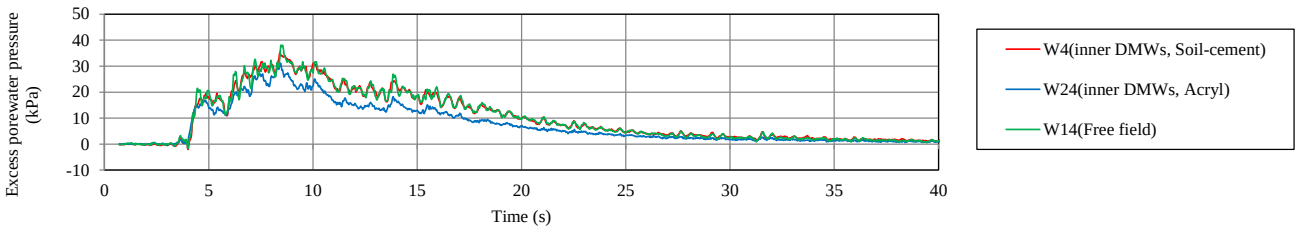

Fig. 4 – Time histories of measured excess pore water pressures (step 5)

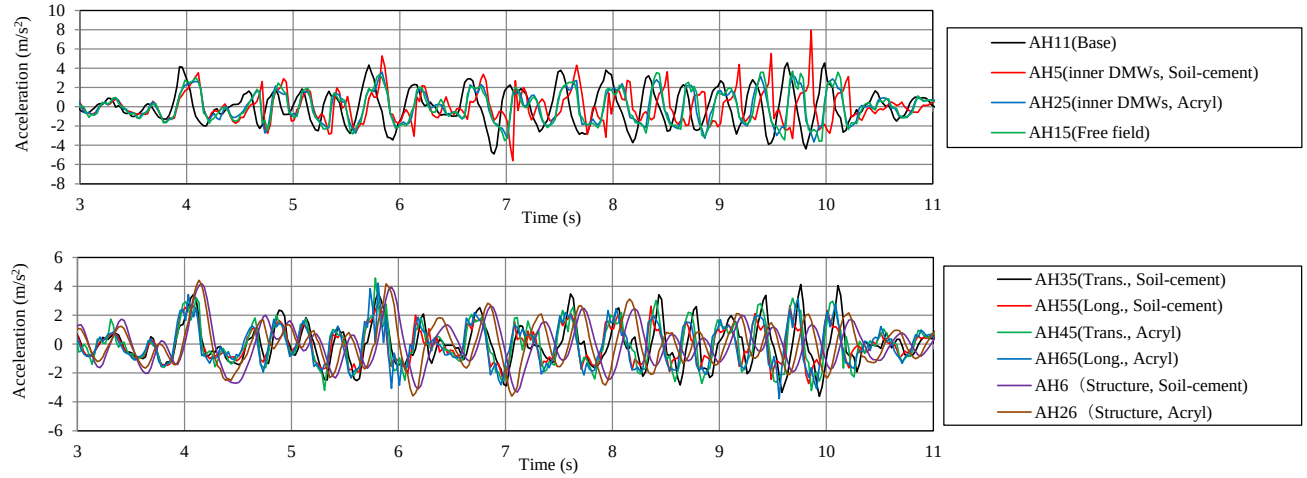

Fig. 5 – Time histories of measured accelerations (step 15)

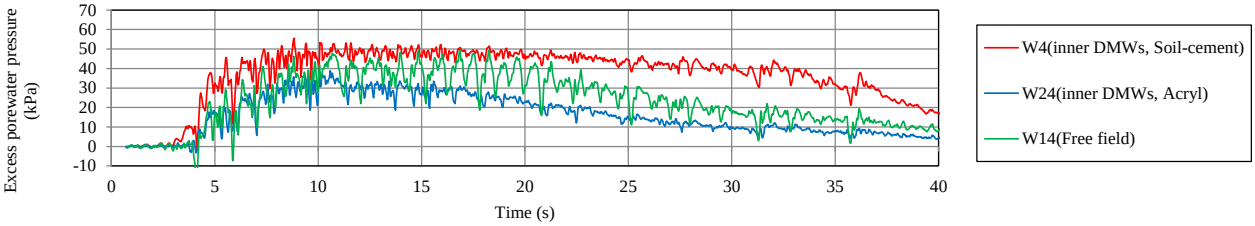

Fig. 6 – Time histories of measured excess pore water pressures (step 15)

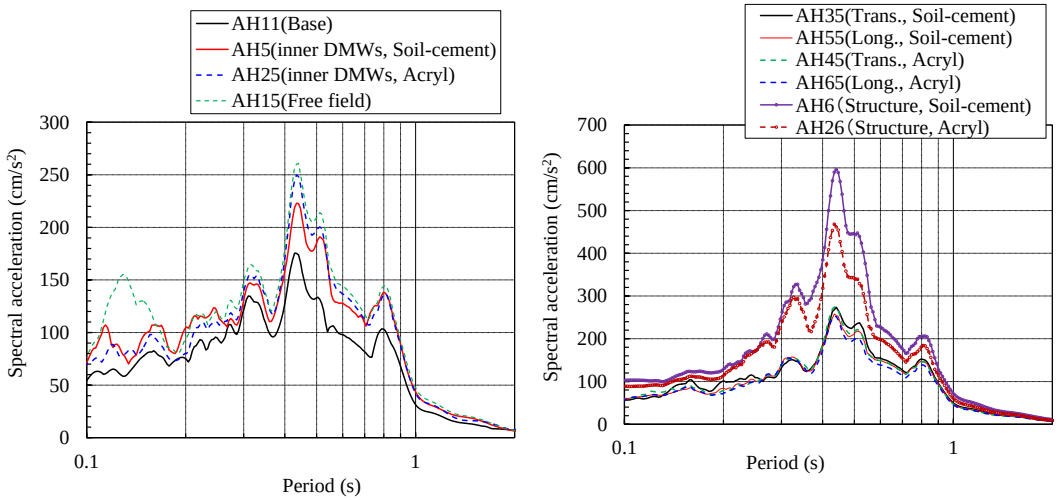

(a) Step 1

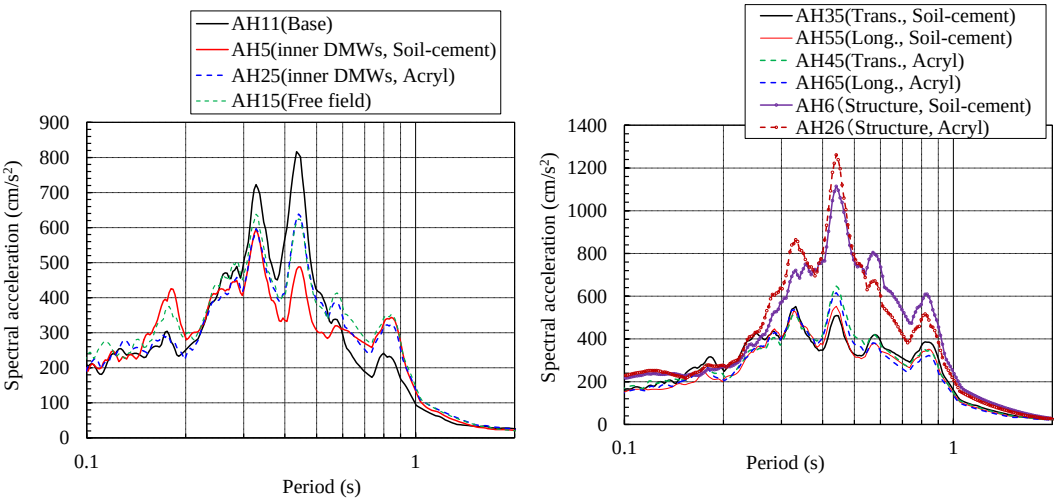

(b) Step 5

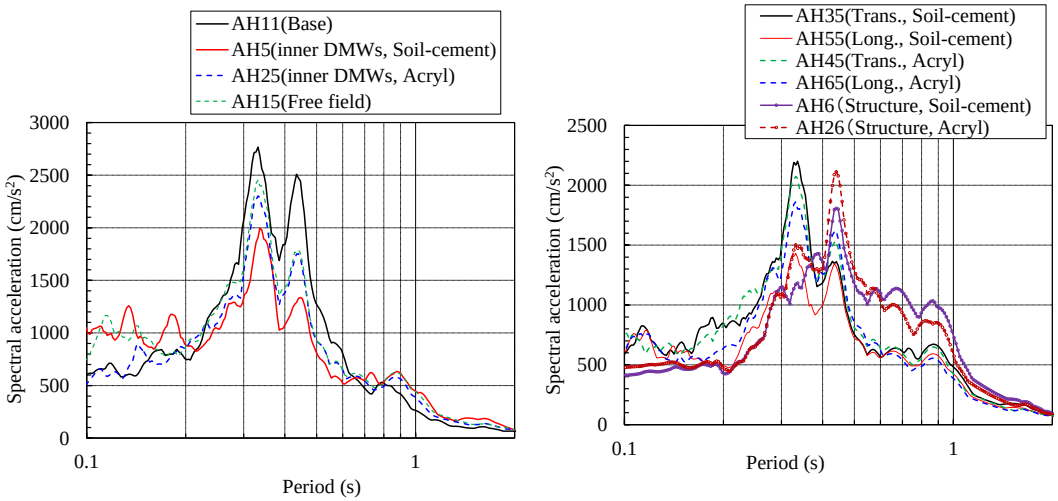

(c) Step 15

Fig. 7 – Acceleration response spectra (5 % damping)

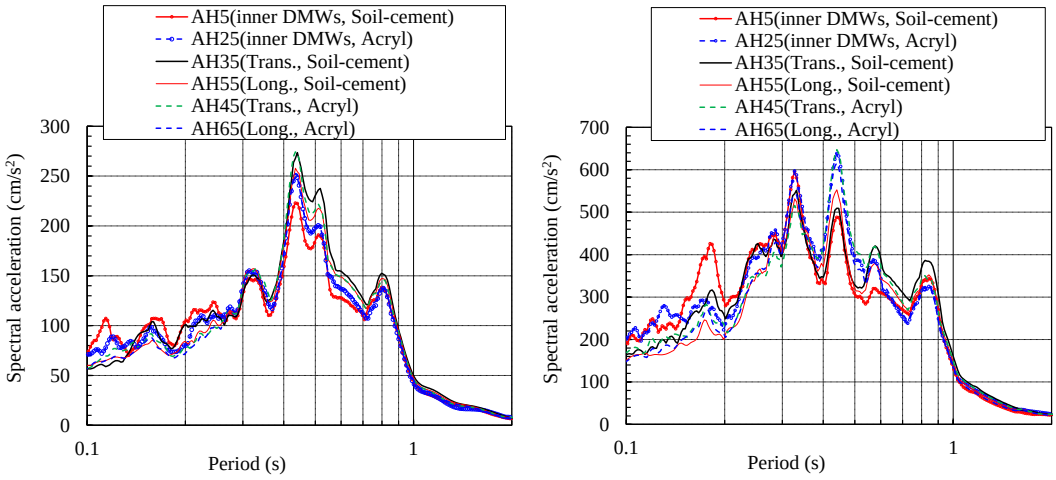

(a) Step1 (b) Step5

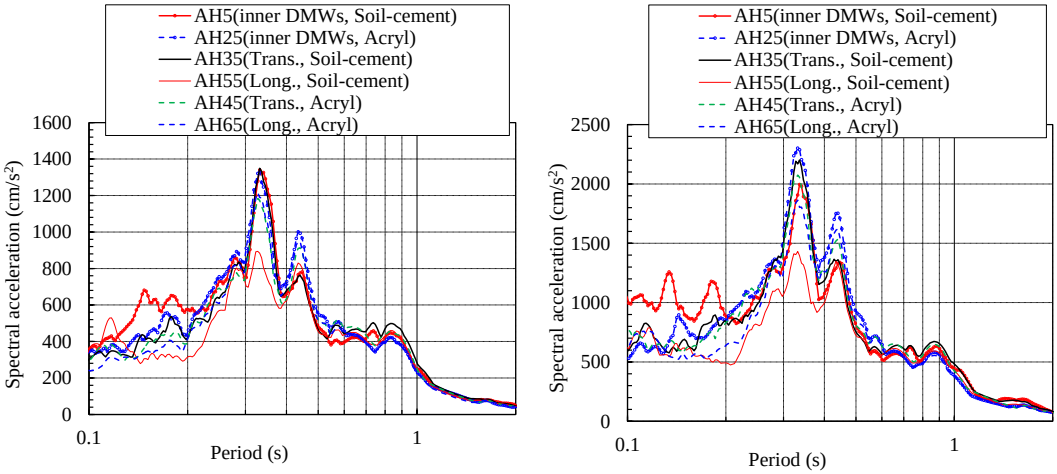

(c) Step10 (d) Step15

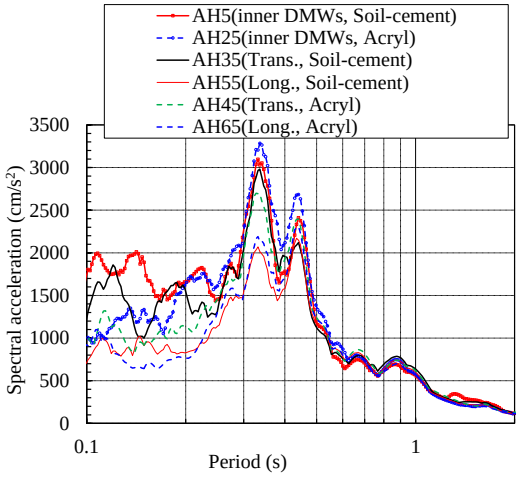

(e) Step18

Fig. 8 – Acceleration response spectra of ground and DMWs (5 % damping)

Figure 9 (a) shows the relationship between the shear strain of the inner ground at the soil-cement model, γ_{eg_soil} and the shear stress of the whole improved ground at the soil-cement model, τ_{eg_soil}. The inertial forces of structure and soil enclosed by the DMWs were assumed to be the lateral load acting on the DMWs. These values are defined as follows:

$$\gamma_{eg\_soil} = (\delta_{AH5} - \delta_{AH2})/h \quad (1)$$

$$\tau_{eg\_soil} = (a_{AH6} \times m_s + a_{AH5} \times m_{g5} + a_{AH4} \times m_{g4} + a_{AH3} \times m_{g3} + a_{AH2} \times m_{g2})/A_{Whole} \quad (2)$$

where δ_{AH**} is a displacement at the point of AH** calculated by double integrations from the measured acceleration of a_{AH**} using the frequency components from 20 Hz to 0.05 Hz; a_{AH**} is an acceleration at the point of AH** shown in Fig.1; h is a distance between accelerometers; m_s is a mass of structure; and $m_{g5\text{-}2}$ is a mass of ground separated to each layer of 5, 4, 3 and 2.

h= 7.5 m

m_s= (2111+1442)= 3553 ton

m_{g5}= 4.25m$\times$ A_{Whole} $\times \rho_s$ = 1458 ton

m_{g4}=m_{g3}= 2.5m$\times$ A_{Whole} $\times$ ρ_s = 857 ton

m_{g2}= 1.75m$\times$ A_{Whole} $\times$ ρ_s = 600 ton

A_{Whole}=13m$\times$13m=169 m^2

ρ_s=2.03 t/m^3

Figure 9 (b) shows the relationship between the shear strain of the inner ground at the acrylic model, γ_{eg_acryl} and the shear stress of the whole improved ground at the acrylic model, τ_{eg_acryl}. These values are defined as follows:

$$\gamma_{eg\_acryl} = (\delta_{AH25} - \delta_{AH22})/h \quad (3)$$

$$\tau_{eg\_acryl} = (a_{AH26} \times m_s + a_{AH25} \times m_{g5} + a_{AH24} \times m_{g4} + a_{AH23} \times m_{g3} + a_{AH22} \times m_{g2})/A_{Whole} \quad (4)$$

Figure 10 (a) shows the relationship between the shear strain of the longitudinal DMWs at the soil-cement model, γ_{DMW_soil} and the assumed shear stress of the longitudinal DMWs at the soil-cement model, τ_{DMW_soil}. It is assumed that lateral load was supported only by two sheets of longitudinal DMWs. These values are defined as follows:

$$\gamma_{DCM\_soil} = (\delta_{AH55} - \delta_{AH52})/h \quad (5)$$

$$\tau_{DCM\_soil} = (a_{AH6} \times m_s + a_{AH5} \times m_{g5} + a_{AH4} \times m_{g4} + a_{AH3} \times m_{g3} + a_{AH2} \times m_{g2})/A_{DMW\_L} \quad (6)$$

where

A_{DMW_L}=13m$\times$1m$\times$2sheets=26 m^2

Figure 10 (b) shows the relationship between the shear strain of the longitudinal DMWs at the acrylic model, γ_{DCM_acryl} and the assumed shear stress of the longitudinal DMWs at the acrylic model, τ_{DCM_acryl}. These values are defined as follows:

$$\gamma_{DCM\_acryl} = (\delta_{AH65} - \delta_{AH62})/h \quad (7)$$

$$\tau_{DCM\_acryl} = (a_{AH26} \times m_s + a_{AH25} \times m_{g5} + a_{AH24} \times m_{g4} + a_{AH23} \times m_{g3} + a_{AH22} \times m_{g2}/A_{DMW\_L} \quad (8)$$

Hyperbolic curves (HD model) estimated by the initial shear stiffness of 800 MPa, and the ultimate shear stress of 1200 kPa (0.3*Fc*, where *Fc*=4000kPa) were also described in Fig. 10. Both the structure models behaved similarly during a small earthquake.

Photo 2 shows the DMW model made of soil-cement after shaking tests. The photos (b), (c), (e) and (g) in Photo 2 show the inside views of the DMWs. A relatively large crack was observed at the longitudinal wall shown each in Photo 2 (a) and (b), the crack near the bottom of the wall shown in Photo 2(b) occurred when the wall was removed after the tests. It is considered that the cracks of the longitudinal walls were caused by the inertial force of structure. Several small cracks were observed not only at longitudinal walls but also at transverse walls. Most of the cracks at transverse walls were observed on the outer plane at the walls as shown in Photo 2(h). It is presumed that some of the cracks in transverse walls were caused by either or both of the deformations of the inner ground enclosed by DMWs and the outside ground. Seismic behaviors of the whole improved ground of the soil-cement model were similar to those of the acrylic model as shown in Fig. 9 even though several cracks were observed.

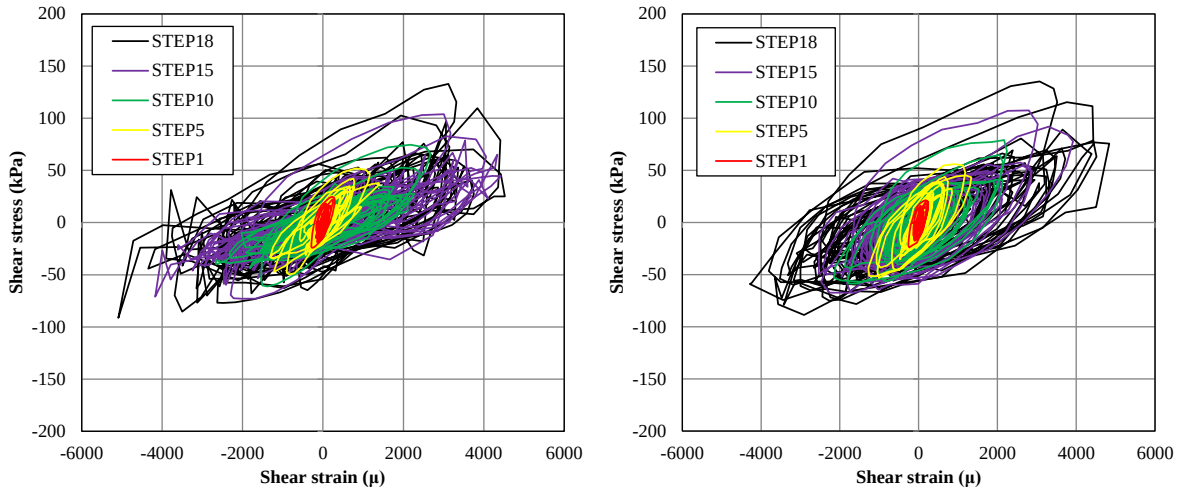

(a) Soil-cement model (b) Acrylic model

Fig. 9 – Relationship between shear strain and shear stress of improved ground in whole

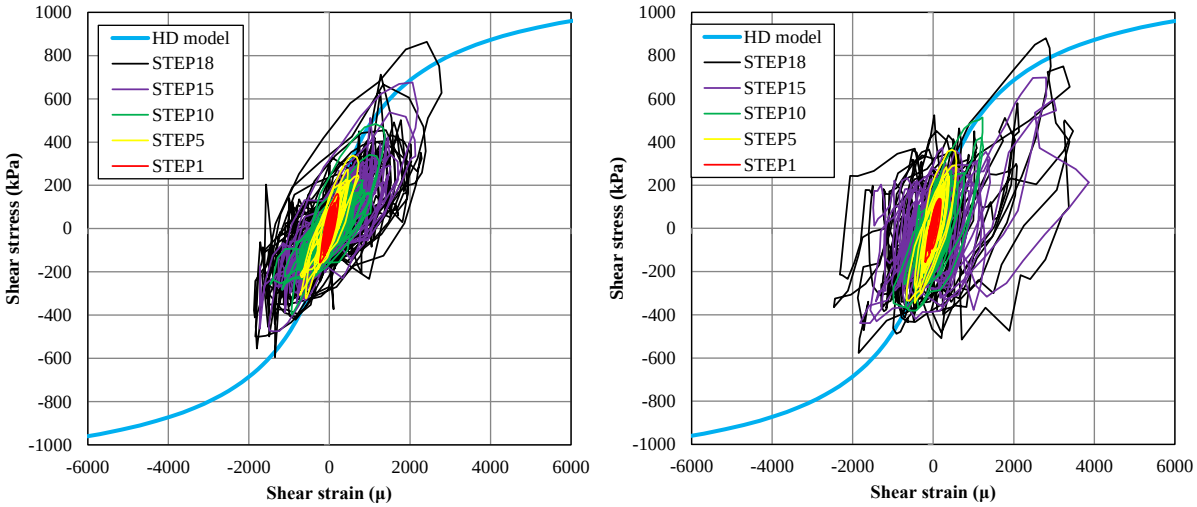

(a) Soil-cement model (b) Acrylic model

Fig. 10 – Relationship between shear strain and assumed shear stress of longitudinal DMWs

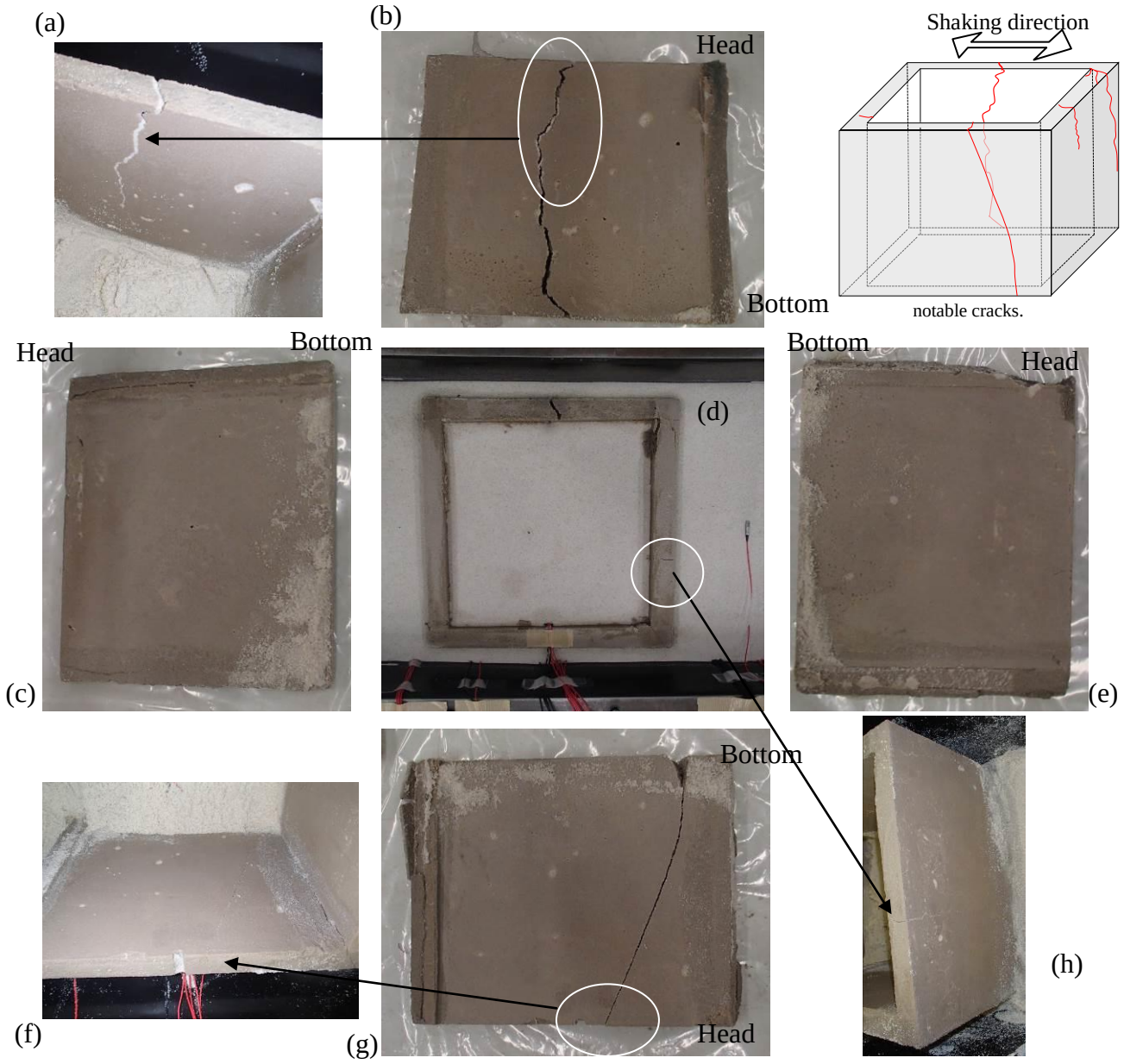

Photo 2 – Observed cracks in DMW model after shaking tests

3. Conclusions

We have carried out a series of centrifuge model tests in 50 g using saturated liquefiable model sand with grid-form deep cement mixing walls in order to investigate the failure behaviors of DMWs subjected to dynamic loading during a large earthquake.

DMW models made by acrylic resin and real soil-cement were simultaneously vibrated to check the shear stiffness of the soil-cement model and degree of yielding of the soil-cement model. Both models behaved similarly when an input acceleration was under 2 m/s^2, and the whole behaviors of improved ground models were similar even though it was over 8 m/s^2. Several cracks of the soil-cement model were observed after repetitive shaking tests including input motion over 8 m/s^2. Those cracks were visually observed. A relatively

large crack occurred at longitudinal walls, and several small cracks were observed at outside of transvers wall. It is considered that the cracks of the longitudinal walls were caused by the inertial force of structure, and the cracks of transverse walls were caused by either or both of the deformations of the inner ground enclosed by DMWs and the outside ground. No significant settlement was observed in the tested structure though the stress reached tensile or shear criteria at a part of the grid-form DMWs.

4. Acknowledgements

The authors are grateful to Mr. N. Nakatsu of Takenaka Corporation for his contributions to the experiments and to Dr. K. Yamashita for help in interpreting the significance of the results of the experiments.

5. References

[1] Tokimatsu, K., Mizuno, H. and Kakurai, M. (1996): Building damage associated with geotechnical problems. *Special Issue of Soils & Foundations*, 219-234.

[2] Yamashita, K., Hamada, J., Onimaru, S. and Higashino, M. (2012): Seismic behavior of piled raft with ground improvement supporting a base-isolated building on soft ground in Tokyo, *Soils & Foundations*, Vol.52, No.5, 1000-1015 Special issue on Geotechnical Aspects of the 2011 off the Pacific coast of Tohoku Earthquake.

[3] Yamashita, K., Hamada, J. and Tanikawa, T. (2016) : Static and seismic performance of a friction piled raft with deep mixing walls in soft ground in Tokyo, *Soil & Foundations* (Accepted).

[4] Namikawa, Y., Koseki, J. and Suzuki, Y. (2007): Finite element analysis of lattice-shaped ground improvement by cement-mixing for liquefaction mitigation, *Soils & Foundations*, Vol.47, No.3, 559-576.

[5] Shigeno, Y., Hamada, J., Yamashita, K. and Nakamura, N. (2017): Numerical analyses of a piled raft foundation with grid-form DMWs under large earthquake load, *16WCEE* (contributing).

[6] Babasaki, R., Suzuki, K. and Suzuki, Y. (1992): Centrifuge tests on improved ground for liquefaction, *Proc. 10th WCEE, Balkema, Rotterdam, Netherlands*, 1461-1464.

[7] Tamura, S., Khosravi, M., Boulanger, R. W., Wilson, D. W., Olgun, C. G., Rayamajhi, D. and Wang, Y. (2015): Site response of soft clay reinforced by soil-cement grid based on dynamic centrifuge tests, *6th International Conference on Earthquake Geotechnical Engineering*.

[8] Khosravi, M., Boulanger, R. W., Tamura, S., Wilson, D. W., Olgun, C. O. and Wang, Y. (2016): Dynamic centrifuge tests of soft clay reinforced by soil-cement grids, *J. Geotech. Geoenviron. Eng.*

[9] Honda, T., Hamada, J. and Nakatsu, N. (2015): Centrifuge model tests on dynamic performance of grid-form soil improvement walls, *50th Annual Convention of Japanese Society of Soil Mechanics and Foundation Engineering*, 1259-1260 (in Japanese).

[10] Hamada, J., Honda, T. and Nakatsu, N. (2016): Dynamic centrifuge model tests on failire behavior of grid-form DMWs supporting a tall building, *Takenaka Technical Research Report*, No.72.